RSC Advances

PAPER

View Article Online
View Journal | View Issue

Cite this: *RSC Adv.*, 2015, **5**, 62982

Fluorescent selectivity for small molecules of three Zn-MOFs with different topologies based on a tetracarboxylate ligand†

Jie Yang,[b] Liangliang Zhang,[a] Xiaoqing Wang,[b] Rongming Wang,[a] Fangna Dai*[a] and Daofeng Sun*[a]

Received 2nd June 2015
Accepted 15th July 2015

DOI: 10.1039/c5ra10391f

www.rsc.org/advances

Three new metal–organic frameworks (MOFs) constructed from terphenyl-3,3″,5,5″-tetracarboxylic acid (H_4ptptc) and zinc nitrate, $[Zn_2(ptptc)(DMF)_3]\cdot 4H_2O\cdot 5.5DMF$ (**1**), $[Zn_2(ptptc)(DMA)(H_2O)]\cdot 2.5H_2O\cdot 3.5DMA$ (**2**) and $[Zn(ptptc)_{0.5}(H_2O)]\cdot DMF\cdot DMA$ (**3**), have been obtained and characterized. All the complexes exhibit 3D 4-connected networks with different topologies involving diamond (**dia**, for **1**), lonsdaleite (**lon**, for **2**) and **Nbo** (for **3**), which emanate from the different reaction solvents (DMF, DMA and mixture of DMF/DMA (1 : 1), respectively). The results of photoluminescence properties show that the three complexes can be act as potential luminescent probes or sensors for detecting small organic molecules and toxic substances.

Introduction

In recent years, the rapid inflation of research efforts related to metal–organic frameworks (MOFs) is ascribed to their interesting topologies and high potential applications in gas adsorption and separation, heterogeneous catalysis, magnetism optical materials and so on.[1–4] It is well known that different building blocks can be self-assembled into infinite arrays, however, the same building blocks also can generate different structures under multiple external elements such as the reaction solvent, pH value, system temperature, and so on.[5–7] Tiny changes of system temperature and pH values can lead to different topologies. For example, two novel temperature-dependent supramolecular stereoisomers of copper coordination networks (**pts** and **NbO**) have been reported by Zhou and coworkers.[8] Three different structural MOFs (MIL-118, MIL-119 and MIL-120)[9] were obtained in the different pH values due that pH value could lead to different deprotonated degrees of ligand. In addition to the system temperature and pH value, solvent effect often plays another important factor on the assembly of reported MOFs. Tzeng group reported three Cd^{II}-networks (1D, 2D, and 3D) based on *S*-spaced-4,4′-bipyridine ligand using the solvent as ligand.[10] When put the solvent as guest, two **pts** and **lvt** topologies were also obtained *via* the reaction of 2,5-bis(pyrazine)-1,3,4-oxadiazole (bpzo) ligand and $AgBF_4$.[11] Therefore, understanding the influential factors of the coordinated structures is very important as it could regulate and control the characteristics of MOFs. On the other hand, environmental issues such as industrial pollution, exhaust emission and pesticide residue become the hot topics attracting lots of public attention.[12] The traditional selective recognition of such small molecules needs expensive instruments and multiple spectrometry as well as intricate characterization approaches.[13] It is an urgent to discover series of materials for selectively recognizing the toxic substances in the environment. There into, according to the reported results, MOF is one of the competitive materials for detecting small molecules, which is considered to be more inexpensive, simplicity and efficient.[14]

In this paper, we choose terphenyl-3,3″,5,5″-tetracarboxylic acid (H_4ptptc) as organic linker for building MOFs based on the reasons as follows: (i) four potential coordination groups and the rigid terphenyl in the tetracarboxylate ligand can afford more coordination opportunities to form diverse structures. (ii) The ligand possesses delocalized π-electron system, which can provide an intense absorbing photosensitizer. (iii) It is favor to form the structures with high symmetry. Herein, three 3D Zn-MOFs: $[Zn_2(ptptc)(DMF)_3]\cdot 4H_2O\cdot 5.5DMF$ (**1**), $[Zn_2(ptptc)(DMA)(H_2O)]\cdot 2.5H_2O\cdot 3.5DMA$ (**2**) and $[Zn(ptptc)_{0.5}(H_2O)]\cdot DMF\cdot DMA$ (**3**) have been obtained through the solvothermal reactions of H_4ptptc and Zn(II) ion in the different solvents (DMF, DMA and mixture of DMF/DMA (1 : 1), respectively). Complexes **1–3** are 4-connected 3D networks with diverse topological structures, which are highly dependent on their reaction solvents. The luminescent properties of complexes **1–3** are measured, and such solvent-dependent luminescence properties are of interest for the sensing of solvent molecules.

[a]*State Key Laboratory of Heavy Oil Processing, China University of Petroleum (East China), College of Science, China University of Petroleum (East China), Qingdao, Shandong, 266580, P. R. China. E-mail: fndai@upc.edu.cn; dfsun@upc.edu.cn*

[b]*Key Lab of Colloid and Interface Chemistry, Ministry of Education School of Chemistry and Chemical Engineering, Shandong University, Jinan, Shandong, 250100, P. R. China*

† Electronic supplementary information (ESI) available. CCDC 1042265, 1042267 and 1042266. For ESI and crystallographic data in CIF or other electronic format see DOI: 10.1039/c5ra10391f

Results and discussion

Crystal structure

X-ray single-crystal diffraction reveals that complex **1** crystallizes in the orthorhombic space group $Pna2_1$, and there are two Zn(II) ions, one ptptc^{4-} ligand and three coordinated DMF molecules in its asymmetric unit. As shown in Fig. 1a, Zn1 displays a distorted octahedral geometry coordinated by three O atoms from three ptptc^{4-} ligands and three O atoms from three coordinated DMF molecules. Zn2 presents the same configuration to Zn1, while the difference is that it is coordinated by six O atoms from four different ligands. The carboxylate groups of ligand adopt three coordination modes: μ_1-η^1:η^1, μ_2-η^2:η^1 and μ_2-η^1:η^1. The distance of Zn1···Zn2 is 3.348 Å and the bond length range of Zn–O is 1.975 (4)–2.422 (4) Å. Viewed from Fig. 1b and c, each binuclear cluster is connected by the backbones of four ptptc^{4-} ligands to generate a 3D open framework. The diagonals of 1D square channel in the 3D framework are about 9.4 Å × 10.3 Å along *b* axis. The calculation of void volume that excluding lattice solvent molecules is 38.9% through the PLATON[15] software. The 3D framework can be clarified as a 4-connected 6^6-**dia** network by considering binuclear cluster and ptptc^{4-} ligand as the 4-connected nodes through the analysis of the TOPOS[16] software, which have been reported in previous literatures.[17] The topology expression is 4/6/c1 (sqc6), and the intricate symbol is [6(2)·6(2)·6(2)·6(2)·6(2)·6(2)] (Fig. 1d).

Complex **2** crystallizes in the monoclinic space group $P2_1$, and the asymmetric unit contains two Zn^{2+} ions, one ptptc^{4-} ligand, one coordinated DMA molecule and one coordinated water molecule. As displayed in Fig. 2a, Zn1 is surrounded by five O atoms from four different ptptc^{4-} ligands to perform a distorted trigonal bipyramidal geometry, Zn2 is also five-coordinated displayed the same geometry, while it is coordinated by one DMA molecule, one water molecule. The carboxylate groups of ptptc^{4-} ligand in **2** adopt two coordination modes: μ_1-η^1:η^1 and μ_2-η^1:η^1), the distance of Zn1···Zn2 is 3.433 Å and the Zn–O bond length range is from 1.945 (3) to 2.390 (3) Å. Each ligand connects four $Zn_2(COO)_4$ SBUs, and each SBU attaches four ptptc^{4-} ligands, generating a 3D opens network with triangle channels along *a* axis (Fig. 2b and c). The void volume after removal of the solvates is 53.9%. Furthermore, Zn-SBU and ptptc^{4-} ligand are 4-connected nodes and both of them connect with each other to form a 6^6-**lon** (4/6/h2) network, and the Schläfli symbol is [6(2).6(2).6(2).6(2).6(2).6(2)] calculated through the analysis of the topology program[18] (Fig. 2d).

Complex **3** crystallizes in the trigonal crystal system with $R\bar{3}m$ space group by analyzing the crystal data. In the asymmetric unit of **3**, there are one Zn^{2+} ion, half of ptptc^{4-} ligand and one water molecule. Each zinc ion is five-coordinated with tetragonal pyramid geometry constructed by four O atoms from four different ptptc^{4-} ligands and O1w from coordinated water molecules (see Fig. 3a). Two zinc ions are bonded by four carboxylate groups adopting a bidentate bridging mode to form the classic Zn(II) paddlewheel secondary building unit (SBU) with a Zn···Zn distance of 2.98 Å. The $[Zn_2(CO_2)_4]$ unit is bridged by four ptptc^{4-} ligands to form a porous framework. The distance of Zn–O1w is 1.977 Å, and the average Zn–$O_{ptptc^{4-}}$ bond distance is 2.023 Å, which are all within the bond length range of Cu(Zn)-paddlewheel complexes.[19] As exhibited in Fig. 3b, there are two types of organometallic cages along the *c* axis. One type of cage is composed of six $Zn_2(COO)_4(H_2O)$ SBUs, the other one consists of twelve $Zn_2(COO)_4(H_2O)$ SBUs, and their diameters are about 5.3 and 9.2 Å, respectively. The total volume is 67.8% for **3**, as obtained by PLATON routine. The TOPOS[16] software illustrates that **3** is a $6^4 \cdot 8^2$ **NbO**-type (4/6/c2, sqc35) topological structure constructed by organic ligands and Zn-SBUs, and the symbol is [6(2)·6(2)·6(2)·6(2)·8(2)·8(2)] (Fig. 3c).

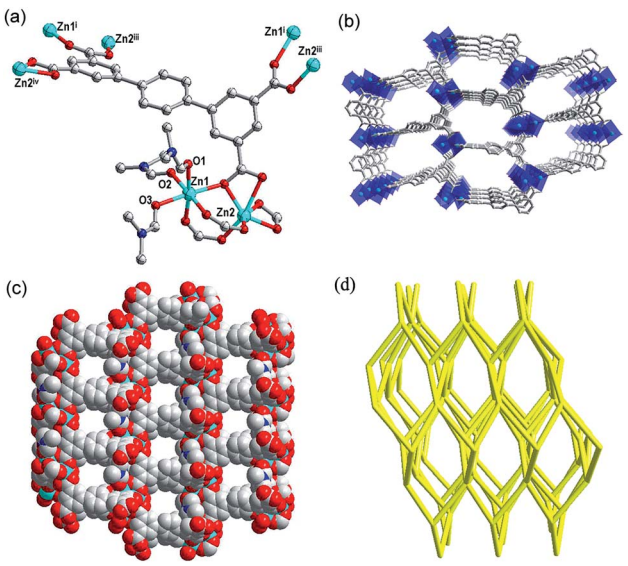

Fig. 1 (a) Coordination environment of the Zn(II) in complex **1**. (b and c) 3D framework viewed from *b* axis and space filling representation viewed from *a* axis. (d) Schematic illustration of the 3D network with **dia** topology.

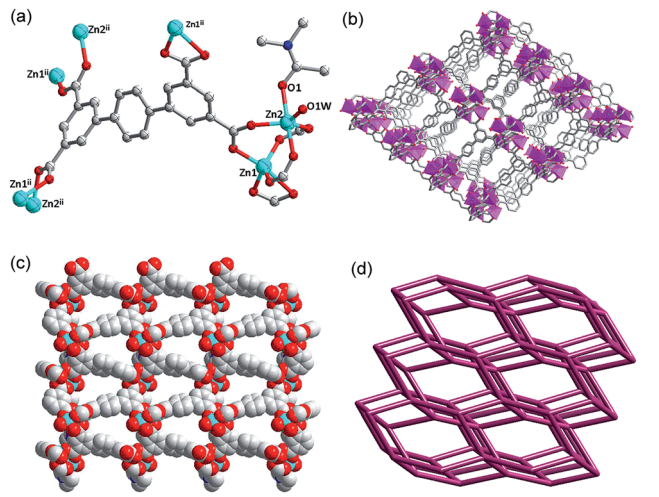

Fig. 2 (a) Coordination environment of the Zn(II) in complex **2**. (b) The 3D framework viewed from *b* axis. (c) Space filling representation viewed from *a* axis. (d) Schematic illustrating 3D network with **lon** topology.

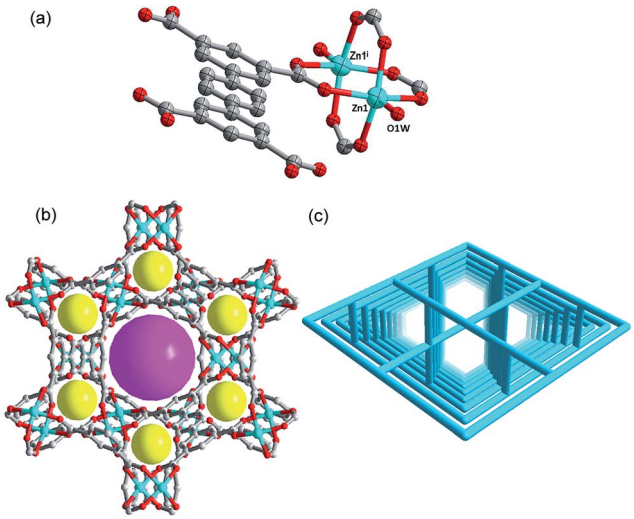

Fig. 3 (a) Coordination environment of the Zn(II). (b) The 3D framework viewed from *c* axis. (c) Schematic illustration of the 3D network with (4,4)-**NbO** topology.

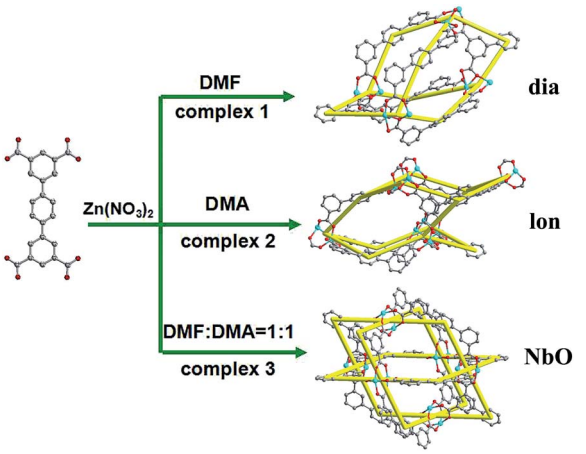

Fig. 4 Solvent-controlled formation of complexes **1–3**.

Effect of solvents on the complexes 1–3

As is well known, the solvent is one of the external factors that influence the formation of MOFs structures.[20] The reaction conditions (ratio of reactants, the system temperature, and reaction time) are the same for the syntheses of complexes **1–3** except for solvents, which results in the formation of different structures and topologies. The formation of **dia**, **lon** and **NbO** networks (Fig. 4) is dependent on the different solvents (DMF, DMA and a mixture of DMF/DMA (1 : 1), respectively) for complexes **1–3**. The reasons of different structures are probably summarized as follows: (1) different solvent molecules may possibly coordinate with metal ions during the synthesis process, which could have structure-directing properties affecting the structures; (2) the dihedral angles between the intermediate benzene ring and adjacent two benzene rings in the $ptptc^{4-}$ ligand for three complexes are different in different solvents. The dihedral angle among the benzene rings in the structure **1** is approximative 32.38° and 36.43°, respectively. The dihedral angle of the structure **2** is about 35.14° and 35.17°, respectively, while the three benzene rings of the organic ligand in complex **3** are almost on the same plane (Fig. S1†).

Powder diffraction measurements and thermal analyses

PXRD has been used to check the purity of the samples in the solid state, and each PXRD pattern of sample is consistent with its simulated one (Fig. S2†). The thermal stability properties of three complexes were performed under N_2 atmosphere at a ramp rate of 10 °C min^{-1} and the temperature ranged from 40 °C to 900 °C. The curves are displayed in ESI Fig. S3.† From the TGA curve of complex **1**, the weight loss at the temperature range from 40 °C to 176 °C is 38.5% (calcd 38.7%) corresponding to the removal of four water molecules and five and a half DMF molecules. After 176 °C, **1** starts to decompose. The thermal stability curve of complex **2** are exhibited weight losses between 40 and 375 °C, which are attributed to the loss of molecules from the pores and decoordination of DMA and water (found 34.1%, calcd 35.4%). The decomposition of **2** starts at 375 °C. For **3**, the 39.7% weight loss (calcd 40.1%) are attributed to the release of one DMF molecule and one DMA molecule at 330 °C. After 330 °C, **3** starts to decompose.

Luminescent properties and fluorescence sensing

The ligand coordinated with d^{10} transition metal centers have exhibited excellent luminescent applications in chemical sensors, luminescent materials and electroluminescent display, and so on.[21] The solid state luminescent spectra for complexes **1–3** and free organic ligand were performed at room temperature. As exhibited in Fig. 5a, the main characteristic peak of free H_4ptptc ligand is observed at 431 nm, which may be ascribed to the $\pi^* \rightarrow n$ or $\pi^* \rightarrow \pi$ transitions.[22] The characteristic emission peaks of complexes **1–3** are exhibited at 403 nm, 406 nm and 399 nm under the same conditions as the excitation wavelength (330 nm) of the free H_4ptptc ligand, which are obvious blue-shifted of 28 nm, 25 nm and 32 nm in comparison with the free ligand, respectively. The different wavelengths of maximum peak among complexes **1–3** may be attributed to the deviations of the coordination modes between the central metal ions and $ptptc^{4-}$ ligand.

In order to explore the sensing sensitivity of complexes **1–3** for solvent molecules, **1–3** and free ligand were dispersed in different solvent emulsions (DMF, CH_3OH, CH_3CN, CH_2Cl_2, acetone, isopropanol and DMSO), and their luminescence intensities were investigated. When free ligand was dispersed in DMF and DMSO, respectively, remarkable blue shifts are observed for the emission of free ligand relative to all the other solvent molecules due to the different solubility (Fig. S8†). As illustrated in Fig. 5b, complex **1** dispersed in isopropanol (i-PrOH) displays the strongest luminescent intensity, and it exhibits the weakest emission in dichloromethane (CH_2Cl_2). While the order of the intensity for **2** and **3** are different from that for **1**. As exhibited in Fig. 5c and d, **2** and **3** display the strongest luminescence intensity in CH_3CN and acetone

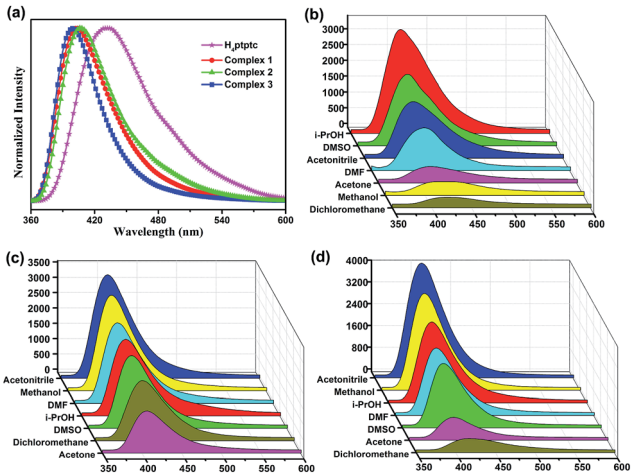

Fig. 5 (a) Room-temperature emission spectra for free ligand and complexes **1–3**. (b–d) The photoluminescence intensities spectra of complexes **1–3** that were dispersed in different organic solvents.

emulsion, respectively, while weakest luminescence intensity is observed in CH_3CN and CH_2Cl_2 emulsion, respectively. The fact that complexes **1–3** exhibit different order of the luminescence intensity may be ascribed to two factors: the different structures and the interactions between the framework and guest solvent molecules. As shown in Fig. S4a,† when complex **1** is dispersed in i-PrOH, the fluorescence intensity gradually decreased with adding amounts of dichloromethane (CH_2Cl_2). A small amount of CH_2Cl_2 can be recognized due to its photoluminescence diminishment, which is dependent on its content. Similar results are observed for complexes **2** and **3**. (Fig. S4b and c†). These intensity differences suggested that the organic molecules could be trapped on the surface of the MOF, which could be attributed into the different interactions between the framework structure and distinct solvents.[12b,24b]

The widespread use of nitro aromatic compounds in industry has seriously harmed the environment and public health due to its high toxicity, therefore, the development of rapid and selective sensing of nitro aromatic compounds is very significant.[23] The 1.0 mM DMSO solution containing different aromatic compounds were added gradually into a batch of DMSO-emulsions of complexes **1–3**, respectively (Fig. S5–7†). To investigate their sensing performances, a series of benzene and nitrobenzene derivatives, such as benzene (BZ), chlorobenzene (CB), nitrobenzene (NB), 4-nitrotoluene (NT), 1,3-dinitrobenzene (1,3-DNB), 2,4-dinitrotoluene (2,4-DNT), 1,4-dinitrobenzene (1,4-DNB) were selected as the analytes. The fluorescence intensities of the DMSO-emulsions of complexes **1–3** reduced gradually upon the addition of different derivatives. In particular, the addition of 1,4-dinitrobenzene shows obvious quenching effect of fluorescence intensity. The quenching percentage after adding the different analytes were calculated *via* the $(I_0 - I)/I_0 \times 100\%$ formula, where I_0 is the initial fluorescence intensity without the benzene and nitrobenzene derivatives, I is the fluorescence intensity after the addition of the derivatives. The sequences of fluorescence quenching percentages in the 0.14 mM concentration of suspension solution for complexes **1–3** are displayed in Fig. 6. The highest fluorescence quenching percentage of complex **1** is 1,4-DNB, which quenches the emission by as much as 41%. The lower quenching efficiencies are observed for other nitrobenzene derivatives and benzene (10%). Complexes **2** and **3** have the similar phenomenons to complex **1**. These results demonstrate a higher selectivity for 1,4-DNB, which can be attributed to the presence of the electron-withdrawing $-NO_2$ groups and electrostatic interactions between 1,4-DNB and the fluorophore.[24,25] Furthermore, to further research the quenching efficiency of the 1,4-DNB for complexes **1–3**, the value of quenching constant K_{sv} are about $5.02 \times 10^3\ M^{-1}$, $4.21 \times 10^3\ M^{-1}$ and $4.36 \times 10^3\ M^{-1}$, respectively, which are calculated by the Stern–Volmer equation, $(I_0/I) = K_{sv}[A] + 1$, [A] is the concentration of the analyte.[26] The above results illustrate that three Zn-MOFs could all serve as the materials detected nitrocompound. Thus, to further design and synthesis of analogous MOFs with the fluorescent sensing properties have become important for environment and public healthiness.

Experimental

Methods

The ligand terphenyl-3,3″,5,5″-tetracarboxylic acid was synthesized through the Suzuki coupling reaction of dibromobenzene and dimethyl-5-(4,4,5,5-tetramethyl-1,3,2-dioxaborolan-2-yl)isophthalate,[27] and reagents used in the synthesis were purchased commercially without further purification. The tests of IR spectra were carried on a Nexus FT-IR Spectrometer ranged in 4000–500 cm^{-1}. C, H, N of elemental analyses were measured on an EA 1110 elemental analyzer. The powder diffraction data were collected on a Cu-Kα radiation using an X-Pert PRO MPD diffractometer. Thermogravimetric analyses were performed in the temperature ranged from 25 to 800 °C with 10 °C min^{-1} rate of heat using a Mettler Toledo TGA instrument. Photoluminescence spectra experiments were obtained on a Hitachi F-7000 spectrofluorometer.

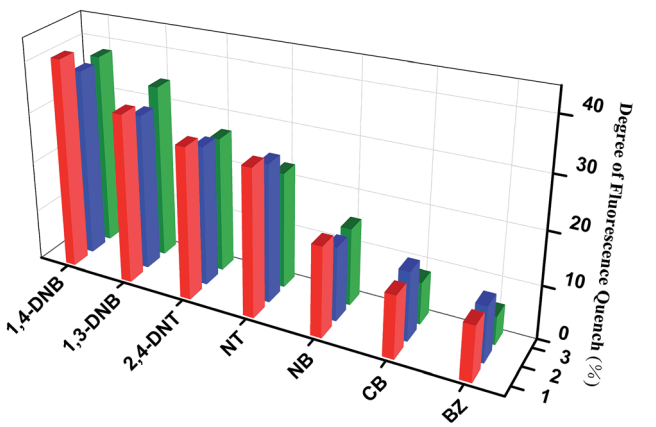

Fig. 6 Percentage of fluorescence quenching obtained for introducing different nitro aromatic compounds into the DMSO-emulsion of complexes **1–3**.

Table 1 Crystal data for complexes **1–3**[a]

Complexes	**1**	**2**	**3**
Formula	$C_{31}H_{31}N_3O_{11}Zn_2$	$C_{26}H_{21}NO_{10}Zn_2$	$C_{11}H_5O_5Zn$
M_r	752.33	638.18	282.52
Crystal system	Orthorhombic	Monoclinic	Trigonal
Space group	$Pna2_1$	$P2_1$	$R\bar{3}m$
a (Å)	18.416 (5)	10.19159 (13)	19.0926 (9)
b (Å)	10.154 (3)	16.42204 (19)	19.0926 (9)
c (Å)	27.010 (8)	15.56239 (19)	37.8155 (15)
α (degree)	90.00	90.00	90.00
β (degree)	90.00	107.0727 (13)	90.00
γ (degree)	90.00	90.00	120.00
Z	4	2	18
V (Å^3)	5051 (2)	2489.85 (5)	11 938.0 (9)
D_c (g cm^{-3})	0.989	0.851	0.707
μ (mm^{-1})	0.991	1.457	0.928
F (000)	1544.0	648.0	2538.0
No. of unique reflns	22 282	39 103	8035
No. of obsd reflns [$I > 2\sigma(I)$]	8783	9434	2575
Parameters	430	355	85
GOF	0.968	1.105	1.130
Final R indices [$I > 2\sigma(I)$]	$R_1 = 0.0606$, w$R_2 = 0.1502$	$R_1 = 0.0427$, w$R_2 = 0.1128$	$R_1 = 0.0703$, w$R_2 = 0.2075$
R Indices (all data)	$R_1 = 0.0753$, w$R_2 = 0.1584$	$R_1 = 0.0467$, w$R_2 = 0.1152$	$R_1 = 0.0856$, w$R_2 = 0.2293$
Largest diff. peak/hole/e Å^{-3}	0.79/−0.47	0.73/−0.45	0.66/−0.74

[a] $R_1 = \sum||F_o| - |F_c||/\sum o|$. w$R_2 = \{\sum[w(F_o^2 - F_c^2)^2]/\sum[w(F_o^2)^2]\}^{1/2}$.

Synthesis of complexes

$[Zn_2(ptptc)(DMF)_3]\cdot 4H_2O\cdot 5.5DMF$ (1). $Zn(NO_3)_2\cdot 6H_2O$ (4.0 mg, 0.014 mmol), H_4ptptc (1.0 mg, 0.0024 mmol) and DMF (1.0 mL) were heated at 90 °C for 3000 min in a sealed glass tube, then yellow crystals were obtained by filtration. Yield: 30%. Calcd for **1**: C, 46.52; H, 6.37; N, 9.70. Found: C, 46.91; H, 6.78; N 9.47. IR (KBr, cm^{-1}): 3434 (m), 1655 (s), 1574 (m), 1382 (m), 1246 (w), 1101 (w), 842 (w), 773 (w), 656 (w).

$[Zn_2(ptptc)(DMA)(H_2O)]\cdot 2.5H_2O\cdot 3.5DMA$ (2). Complex **2** was obtained according to the methods of the complex **1**, and the difference is that the DMA was replaced into the DMF as solvent. Yield: 28%. Calcd for **2**: C, 48.62; H, 5.86; N, 6.38. Found: C, 48.27; H, 5.98; N 6.82. IR (KBr, cm^{-1}): 3354 (m), 2027 (w), 1653 (s), 1387 (m), 1109 (w), 1034 (w), 918 (w), 780 (w), 728 (w), 668 (w), 596 (w).

$[Zn(ptptc)_{0.5}(H_2O)]\cdot DMF\cdot DMA$ (3). Complex **3** was obtained according to the methods of the complex **1**, and the difference is that the DMF : DMA = 1 : 1 was replaced into the DMF as solvent. Yield: 35%. Calcd for **3**: C, 48.61; H, 5.21; N, 6.30. Found: C, 48.86; H, 5.37; N 5.92. IR (KBr, cm^{-1}): 3433 (m), 2019 (w), 1632 (s), 1450 (w), 1398 (m), 1193 (w), 1122 (w), 1023 (m), 711 (w), 602 (w), 593 (w), 479 (w).

Structural crystallography

The X-ray datum of complex **1** was collected on a Bruker APEXII CCD with Mo-Kα radiation ($\lambda = 0.71073$ Å) at room temperature. The data of complexes **2** and **3** were obtained on an Agilent Super nova with Cu-Kα and Mo-Kα radiation ($\lambda = 1.54178$ and 0.71073 Å) at 200 and room temperature, respectively. The absorption corrections were decided by employing the SADABS program.[28] The structures and hydrogen atoms of three complexes were refined to utilize the SHELX-97 program[29] through the full-matrix least-squares by fitting on F^2 and anisotropic thermal parameters, respectively. There are many disordered solvent molecules could existed in the cavity of three complexes, which can be not be achieved through the reasonable modeling. Hence, the diffuse electron could be removed by the PLATON/SQUEEZE routine.[15] The summary of three structures data were displayed in Table 1, and the part of the bond lengths and bond angles were exhibited in Table S1–S3 from ESI.† Three CIF data were confirmed by employing the checkCIF/PLATON service, ESI.†

Conclusions

In summary, three 3D Zn-MOFs: $[Zn_2(ptptc)(DMF)_3]\cdot 4H_2O\cdot 5.5DMF$ (**1**), $[Zn_2(ptptc)(DMA)(H_2O)]\cdot 2.5H_2O\cdot 3.5DMA$ (**2**), $[Zn(ptptc)_{0.5}(H_2O)]\cdot DMF\cdot DMA$ (**3**) based on H_4ptptc and $Zn(NO_3)_2$ have been successfully obtained. Complexes **1–3** are all 3D 4-connected networks, but features different topological structures. These results show that the structures of three MOFs can be affected by the choice of reaction solvent. Choosing DMF gives rise to a **dia** topology for complex **1**, choice of DMA brings about the formation of complex **2** with **lon** network, and using DMF/DMA (1 : 1) leads to the structure of complex **3** with a **NbO** net. Furthermore, the fluorescent recognition properties for three Zn-MOFs were investigated at room temperature. Our study on their guest-free forms exposes that complexes **1–3** could selectively detect dichloromethane (CH_2Cl_2), acetone and CH_2Cl_2 due to the quenching phenomena, respectively. And three complexes were measured for sensing a series of aromatic

compounds. The results illustrate that three complexes exhibit the highest quenching behavior upon adding in a solvent of 1,4-DNB compounds. Further studies will be focused on their recognition selectivity for other functional groups of aromatic compounds, which can explore their application in sensing organic molecule and pollutants. To realize these aims are underway.

Acknowledgements

This work was supported by the NSFC (Grant Nos 21271117, 21201179), the China Postdoctoral Science Foundation funded project (2012M510106, 2014T70665), and the Fundamental Research Funds for the Central Universities (13CX05015A, 14CX02213A).

Notes and references

1 (*a*) M. Kurmoo, *Chem. Soc. Rev.*, 2009, **38**, 1353; (*b*) D. F. Weng, Z. M. Wang and S. Gao, *Chem. Soc. Rev.*, 2011, **40**, 3157.

2 (*a*) J. R. Li, R. J. Kuppler and H. C. Zhou, *Chem. Soc. Rev.*, 2009, **38**, 1477; (*b*) S. Kitagawa and K. Uemura, *Chem. Soc. Rev.*, 2005, **34**, 109.

3 (*a*) S. Kitagawa, R. Kitaura and S. Noro, *Angew. Chem., Int. Ed.*, 2004, **43**, 2334; (*b*) Y. He, S. Xiang and B. Chen, *J. Am. Chem. Soc.*, 2011, **133**, 14570.

4 (*a*) L. Ma, C. Abney and W. Lin, *Chem. Soc. Rev.*, 2009, **38**, 1248; (*b*) J. Y. Lee, O. K. Farha, J. Roberts, K. A. Scheidt, S. T. Nguyen and J. T. Hupp, *Chem. Soc. Rev.*, 2009, **38**, 1450.

5 (*a*) C. K. Brozek, L. Bellarosa, T. Soejima, T. V. Clark, N. López and M. Dincă, *Chem.–Eur. J.*, 2014, **20**, 6871; (*b*) C. P. Li, J. M. Wu and M. Du, *Chem.–Eur. J.*, 2012, **18**, 12437.

6 (*a*) M. Du, X. J. Zhao and Y. Wang, *Dalton Trans.*, 2004, 2065; (*b*) Y. F. Han, W. G. Jia, W. B. Yu and G. X. Jin, *Chem. Soc. Rev.*, 2009, **38**, 3419; (*c*) Y. P. He, Y. X. Tan, F. Wang and J. Zhang, *Inorg. Chem.*, 2012, **51**, 1995; (*d*) D. C. Zhong, W. X. Zhang, F. L. Cao, L. Jiang and T. B. Lu, *Chem. Commun.*, 2011, **47**, 1204; (*e*) J. S. Hu, L. Qin, M. D. Zhang, X. Q. Yao, Y. Z. Li, Z. J. Guo, H. G. Zheng and Z. L. Xue, *Chem. Commun.*, 2012, **48**, 681.

7 (*a*) I. H. Park, R. Medishetty, J. Y. Kim, S. S. Lee and J. Vittal, *Angew. Chem., Int. Ed.*, 2014, **53**, 5591; (*b*) P. P. Cui, J. L. Wu, X. L. Zhao, D. Sun, L. L. Zhang, J. Guo and D. F. Sun, *Cryst. Growth Des.*, 2011, **11**, 5182; (*c*) P. Hu, L. Ma, K. J. Tan, H. Jiang, F. X. Wei, C. H. Yu, K. P. Goetz, O. D. Jurchescu, L. E. McNeil, G. G. Gurzadyan and C. Kloc, *Cryst. Growth Des.*, 2014, **14**, 6376–6382.

8 D. F. Sun, Y. X. Ke, T. M. Mattox, B. A. Ooro and H. C. Zhou, *Chem. Commun.*, 2005, 5447.

9 C. Volkringer, T. Loiseau, N. Guillou, G. Férey, M. Haouas, F. Taulelle, E. Elkaim and N. Stock, *Inorg. Chem.*, 2010, **49**, 9852.

10 B. C. Tzeng, H.-T. Yeh, T.-Y. Chang and G.-H. Lee, *Cryst. Growth Des.*, 2009, **9**, 2552.

11 M. Du, X.-J. Zhao, J.-H. Guo and S. R. Batten, *Chem. Commun.*, 2005, 4836.

12 (*a*) Y. J. Cui, Y. F. Yue, G. D. Qian and B. L. Chen, *Chem. Rev.*, 2012, **112**, 1126; (*b*) X. F. Zheng, L. Zhou, Y. M. Huang, C. G. Wang, J. G. Duan, L. L. Wen, Z. F. Tian and D. F. Li, *J. Mater. Chem. A*, 2014, **2**, 12413; (*c*) H. H. Li, W. Shi, K. N. Zhao, Z. Niu, H. M. Li and P. Cheng, *Chem.–Eur. J.*, 2013, **19**, 3358.

13 (*a*) K. Sumida, D. L. Rogow, J. A. Mason, T. M. McDonald, E. D. Bloch, Z. R. Herm, T. H. Bae and J. R. Long, *Chem. Rev.*, 2012, **112**, 724; (*b*) J. M. Zhou, W. Shi, N. Xu and P. Cheng, *Inorg. Chem.*, 2013, **52**, 8082; (*c*) S. R. Zhang, D. Y. Du, J. S. Qin, S. J. Bao, S. L. Li, W. W. He, Y. Q. Lan, P. Shen and Z. M. Su, *Chem.–Eur. J.*, 2014, **20**, 3589.

14 (*a*) L. E. Kreno, K. Leong, O. K. Farha, M. Allendorf, R. P. Van Duyne and J. T. Hupp, *Chem. Rev.*, 2012, **112**, 1105; (*b*) A. Lan, K. Li, H. Wu, D. H. Olson, T. J. Emge, W. Ki, M. Hong and J. Li, *Angew. Chem., Int. Ed.*, 2009, **48**, 2334; (*c*) S. Pramanik, C. Zheng, X. Zhang, T. J. Emge and J. Li, *J. Am. Chem. Soc.*, 2011, **133**, 4153; (*d*) C. Zhang, Y. Che, Z. Zhang, X. Yang and L. Zang, *Chem. Commun.*, 2011, **47**, 2336; (*e*) Z. Zhang, S. Xiang, X. Rao, Q. Zheng, F. R. Fronczek, G. Qian and B. Chen, *Chem. Commun.*, 2010, **46**, 7205; (*f*) A. K. Chaudhari, S. S. Nagarkar, B. Joarder and S. K. Ghosh, *Cryst. Growth Des.*, 2013, **13**, 3716.

15 (*a*) A. L. Spek, *Platon, A Multipurpose Crystallographic Tool*, Utrecht University, Utrecht, The Netherlands, 1998; (*b*) A. L. Spek, *Acta Crystallogr.*, 2009, **65**, 148.

16 V. A. Blatov, *Struct. Chem.*, 2012, **23**, 955.

17 (*a*) Q. Q. Guo, C. Y. Xu, B. Zhao, Y. Y. Jia, H. W. Hou and Y. T. Fan, *Cryst. Growth Des.*, 2012, **12**, 5439; (*b*) Z. Q. Shi, Y. Z. Li, Z. J. Guo and H. G. Zheng, *Cryst. Growth Des.*, 2013, **13**, 3078.

18 (*a*) L. Wen, P. Cheng and W. B. Lin, *Chem. Sci.*, 2012, **3**, 2288; (*b*) J. Zhang, F. Wang, D. C. Hou, H. Yang, Y. Kang and J. Zhang, *Dalton Trans.*, 2014, **43**, 3210.

19 (*a*) M. Xue, G. S. Zhu, Y. X. Li, X. J. Zhao, Z. Jin, E. H. Kang and S. L. Qiu, *Cryst. Growth Des.*, 2008, **4**, 2478; (*b*) B. Zheng, Z. Q. Liang, G. H. Li, Q. S. Huo and Y. L. Liu, *Cryst. Growth Des.*, 2010, **10**, 3405.

20 (*a*) L. Delhaye, A. Ceccato, P. Jacobs, C. Kottgen and A. Merschaert, *Org. Process Res. Dev.*, 2007, **11**, 160; (*b*) K. M. Kadish, L. L. Wang, A. Thuriere, L. Giribabu, R. Garcia, E. V. Caemelbecke and J. L. Bear, *Inorg. Chem.*, 2003, **42**, 8309.

21 (*a*) X. Shi, G. Zhu, Q. Fang, G. Wu, G. Tian, R. Wang, D. Zhang, M. Xue and S. Qiu, *Eur. J. Inorg. Chem.*, 2004, **1**, 185; (*b*) X. M. Zhang, M. L. Tong, M. L. Gong and X. M. Chen, *Eur. J. Inorg. Chem.*, 2003, **1**, 138; (*c*) L. Wen, Y. Li, Z. Lu, J. Lin, C. Duan and Q. Meng, *Cryst. Growth Des.*, 2006, **6**, 530.

22 (*a*) Y. Yang, P. Du, J. F. Ma, W. Q. Kan, B. Liu and J. Yang, *Cryst. Growth Des.*, 2011, **11**, 5540; (*b*) W. G. Lu, J. H. Deng and D. C. Zhong, *Inorg. Chem. Commun.*, 2012, **20**, 312; (*c*) L. Wen, Z. Lu, J. Lin, Z. Tian, H. Zhu and Q. Meng, *Cryst. Growth Des.*, 2007, **7**, 93; (*d*) J. G. Lin, S. Q. Zang, Z. F. Tian, Y. Z. Li, Y. Y. Xu, H. Z. Zhu and Q. J. Meng, *CrystEngComm*, 2007, **9**, 915.

23 (*a*) F. Arduini, F. Ricci, C. S. Tuta, D. Moscone, A. Amine and G. Palleschi, *Anal. Chim. Acta*, 2006, **580**, 155; (*b*) B. X. Li, Y. Z. He and C. L. Xu, *Talanta*, 2007, **72**, 223; (*c*) X. H. Li, Z. H. Xie, H. Min, Y. Z. Xian and L. T. Jin, *Electroanalysis*, 2007, **24**, 2257.

24 (*a*) S. S. Nagarkar, B. Joarder, A. K. Chaudhari, S. Mukherjee and S. K. Ghosh, *Angew. Chem., Int. Ed.*, 2013, **52**, 2881; (*b*) G. L. Liu, Y. J. Qin, L. Jing, G. Y. Wei and H. Li, *Chem. Commun.*, 2013, **49**, 1699.

25 S. Pramanik, C. Zheng, X. Zhang, T. J. Emge and J. Li, *J. Am. Chem. Soc.*, 2011, **133**, 4153.

26 A. Ganguly, B. K. Paul, S. Ghosh, S. Kar and N. Guchhait, *Analyst*, 2013, **138**, 6532.

27 X. Lin, J. H. Jia, X. B. Zhao, K. M. Thomas, A. J. Blake, G. S. Wallker, N. R. Champness, P. Hubberstey and M. Schröder, *Angew. Chem., Int. Ed.*, 2006, **45**, 7358.

28 G. M. Sheldrick, *SADABS 2.05*, University of Gottingen, Gottingen, Germany, 2002.

29 G. M. Sheldrick, *SHELXS-97, Programs for X-ray Crystal Structure Solution*, University of Gottingen, Gottingen, Germany, 1997.

